UAS mapping of surface roughness and digital grain size to assess pre-dam removal baseline conditions along the mainstem Klamath River corridor below Iron Gate Dam, California

Jennifer A. Curtis, Research Geologist, U.S. Geological Survey, jacurtis@usgs.gov
Jacob J. Taylor, Hydrologic Technician, U.S. Geological Survey
Michael Bartley, Hydrologic Technician, U.S. Geological Survey
Christian Estrada, Physical Scientist, U.S. Geological Survey
Patrick Haluska, Hydrologist, U.S. Geological Survey
Sierra Keller, Hydrologic Technician, U.S. Geological Survey

Abstract

Bed roughness and grain size in river corridors are fundamental indicators of fluvial processes and river hydraulics. In hydraulic models for coarse-grained rivers, the bed roughness height (k) is often assumed to be related to a representative diameter, such as the grain size representing the 84th percentile. This paper presents a workflow for using UAS (Uncrewed Aircraft System) imagery and Structure-from-Motion (SfM) photogrammetry to map surface roughness and digital grain size (DGS) on exposed alluvial bars. In June of 2022, UAS surveys were collected at 7 repeat monitoring sites along the main stem of the lower Klamath River corridor downstream from Iron Gate Dam. The UAS surveys are part of a larger effort to monitor river response to a temporary large-magnitude increase in fine-sediment flux during and following dam removal in 2024. One of the advantages of UAS-SfM methods compared to other high-resolution survey methods is the ability to easily collect imagery at multiple spatial scales. In this study, UAS imagery was collected at three altitudes (high ~60 m, mid~30 m, and low~6 m), and a workflow for creating georeferenced surface roughness maps at the patch (1,000 m^2) to reach (100,000 m^2) scale was developed. Digital Elevation Models (DEMs) and orthomosaics were created using AgiSoft Metashape Professional software and standardized SfM methods. The DEMs were detrended to remove localized bedform gradients and reach slopes. Surface-roughness maps were computed using the standard deviation of detrended elevations within a 1-meter grid. The Portuguese Creek reach was selected for a proof-of-concept DGS, using the low-altitude datasets. Twelve plots for DGS were randomly selected and clipped from the orthomosaic. Grain-size percentiles (5, 10, 16, 25, 32, 75, 84, 90, 95) and statistical metrics (mean, sorting, skewness, kurtosis) were computed using a wavelet method (pyDGS) that requires scaling but does not require site calibration. Study results indicated that surface-roughness maps at all three altitudes provided grain-scale detail suitable for assessing surface roughness variations related to grain size. The mid-altitude survey provided orthomosaics suitable for heads-up digitizing of coarse- and fine-sediment facies. The low-altitude survey provided hyper-resolution (1.5 to 2.5 mm) orthomosaics suitable for DGS of fine-gravel particles ≥ 8 mm. The resolution of the orthomosaic truncates the grain-size distributions and constrains the 5th percentile. Regression models indicated positive correlations between surface roughness and characteristic grain-size percentiles indicating surface roughness can be used as a surrogate metric for grain size when mapping bed textures in river corridors. The UAS-SfM and DGS methods were most appropriate for determining relative differences rather than computing absolute estimates of grain size. This study produced hyper-resolution photogrammetric products with grain-scale detail for reach-scale extents. These close-range, remote-sensing methods can be used for rapid assessment of textural changes in bed sediment and characterization of bed fining in exposed areas of the river corridor during and following dam removal. The methods are fast, non-destructive, repeatable, and transferable.

Introduction

Dam removal in the Klamath River basin (Figure 1), scheduled to be completed in 2024, will constitute the largest dam removal to date and one of the largest ecosystem restorations in U.S. history. The reservoirs impounded in the hydroelectric reach contain approximately 10-12 million cubic meters of mostly fine sediment (>85% silt and clay). During and following dam removal, the fate and transport of reservoir sediment in downstream reaches will depend upon the nature of the reservoir sediments, existing conditions in the downstream river corridor, and the magnitude and duration of instream flows. Approximately 1/3-2/3 of the stored sediment is expected to be released downstream (Reclamation, 2011); the remainder is expected to remain in place and become stabilized by native vegetation.

Downstream from the hydroelectric reach, the Klamath River is a semi-alluvial, coarse-grained river that flows through a steep, narrow, and confined channel (Curtis et al., 2021). During and following dam removal, and depending upon the hydrology, fine sediment is expected to travel rapidly through the lower river to the Pacific Ocean and be dispersed by ocean currents (Reclamation, 2011). Sand and larger-diameter material are expected to be transported downstream more slowly. Deposition and stranding of reservoir sediment along the main-stem river corridor may temporarily increase the proportion of fine sediment stored in downstream reaches and result in textural changes and bed fining.

Bed roughness and grain size are fundamental indicators of fluvial processes and two of the primary variables used to parameterize hydraulic and sediment transport models (Bunte and Abt, 2001; Powell, 2014). In hydraulic models for coarse-grained rivers, the bed roughness height (k) is often assumed to be related to a representative grain diameter such as the grain size representing the 84th percentile (Hey, 1979; van Rijn, 1984; Lane, 2005; Chen et al., 2020). In this study, we define surface roughness as the variance in vertical roughness heights computed as the standard deviation of locally detrended elevations (σ_z) using a Digital Elevation Model (DEM). Digital Grain Size (DGS), or photo-sieving, is defined as an estimate of the grain-size distribution computed from a 2D digital image.

Surface roughness is a scale-dependent parameter that describes the variance in vertical roughness heights across an area of interest (Smith, 2014). Surface roughness maps, derived from Uncrewed Aerial System (UAS) imagery collected at different altitudes, will have different spatial resolutions and roughness amplitudes. Roughness maps computed using higher-altitude imagery will have coarser resolutions, lower roughness amplitudes, smoother textures, and smaller roughness heights. Selecting an appropriate flight altitude for UAS imagery collection and resolution for photogrammetric products is a difficult and critical consideration *(*Groom et al., 2019*)*.

In comparison to other high-resolution survey methods such as terrestrial Light Detection And Ranging (LiDAR), pixel-based methods are preferable for grain-scale studies. Imagery for UAS-SfM can be collected at multiple spatial scales with little additional effort, and the methods easily provide photogrammetric products with sub-centimeter accuracy at the patch (1,000 m^2) to reach (100,000 m^2) scale. UAS surveys can provide hyper-resolution digital products with grain-scale detail for reach-scale extents (Brasington et al., 2012) for areas that are difficult to assess or too large to map using ground-based methods.

UAS-SfM photogrammetry and DGS are particularly well-suited for rapidly detecting changes in bed-sediment textures during and following Klamath River dam removal. Numerous empirical

studies (Smart et al., 2004; Brasington et al., 2012; Westoby et al., 2015; Pearson et al., 2017, Bertin et al., 2018) have shown a strong, positive correlation between vertical roughness height and grain size, indicating surface roughness computed as the standard deviation of detrended bed elevations is a useful surrogate metric for grain size. In coarse-grained rivers, the collection of grain-size data typically relies upon time-consuming and laborious field measurements (Wolman, 1954; Bunte and Abt, 2001). In comparison, UAS surface-roughness mapping and DGS methods are fast, non-destructive, and repeatable methods for monitoring surface textures and grain size in exposed areas of river corridors.

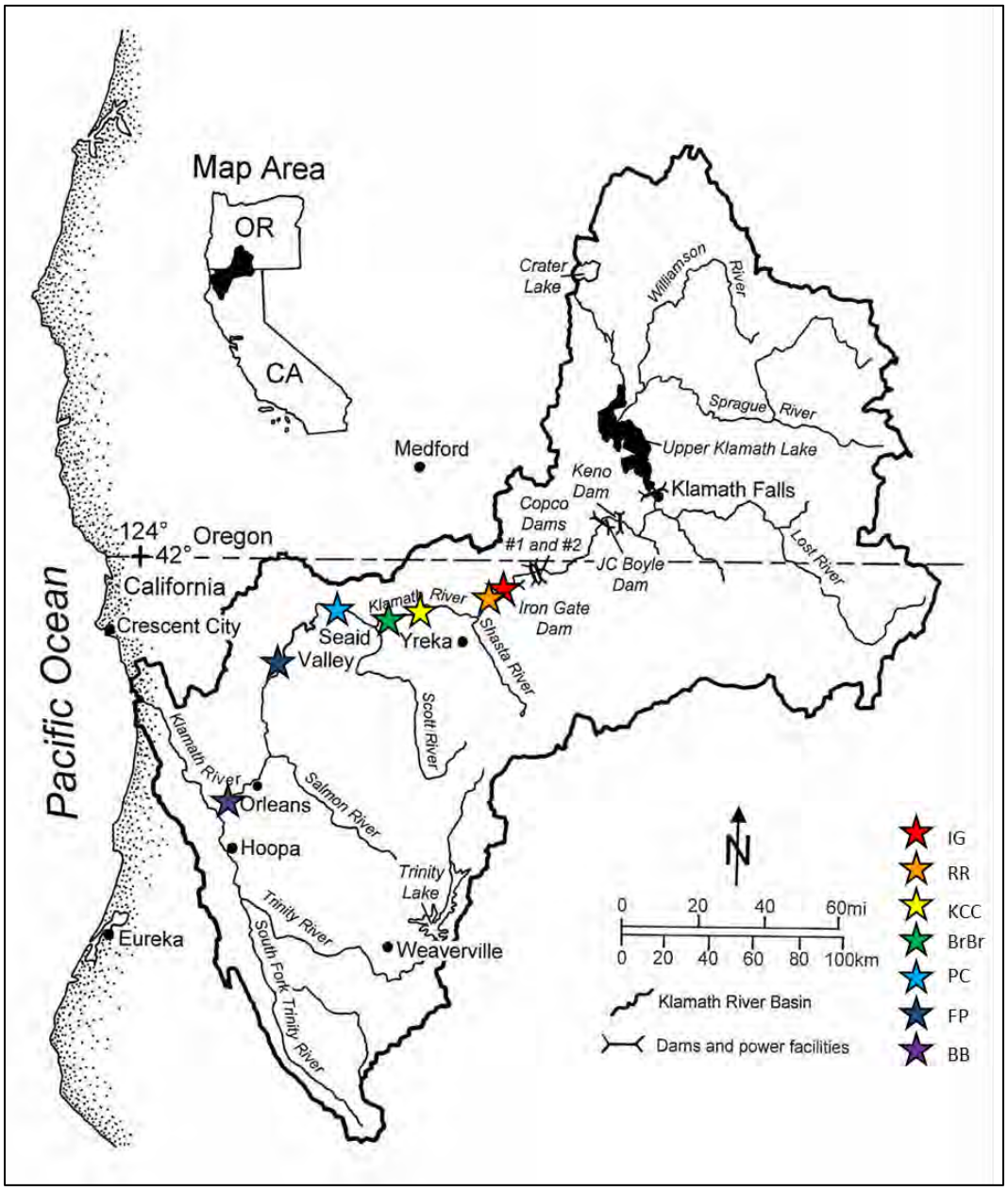

Figure 1. Map of the Klamath River basin showing UAS survey locations (Table 1) along the mainstem Klamath River corridor. Study sites are downstream from four hydroelectric dams that will be removed in 2024 and two diversion dams that will remain in place. Figure modified from Holmquist-Johnson and Milhous (2010)

Objectives

The objective of this pilot study was to evaluate the use of UAS for mapping surface roughness and computing DGS on exposed alluvial bars at repeat monitoring sites along the mainstem Klamath River corridor downstream from Iron Gate Dam. We also evaluated the feasibility of using surface roughness as a surrogate metric for monitoring surface texture and grain size changes on exposed alluvial bars during and following dam removal. Results were further assessed to determine the appropriate UAS flight altitude, spatial scale, and photogrammetric product resolution for detecting changes in surface roughness and DGS.

Because surface roughness is scale-dependent, change detection and longitudinal comparisons among monitoring sites will require consistency in scale, resolution, and post-processing methods. This paper presents a standardized workflow for mapping surface roughness and DGS. This work is part of a larger U.S. Geological Survey (USGS) effort that aims to develop new methods to assess baseline conditions and monitor the physical response of the river corridor to dam removal (https://www.usgs.gov/centers/california-water-science-center/science/klamath-dam-removal-studies).

Study Area

The Klamath River flows from its headwaters in south-central Oregon through northern California to its estuary (Figure 1). A series of hydroelectric facilities (JC Boyle, Copco No. 1, Copco No. 2, and Iron Gate), owned and operated by PacifiCorp (Portland, Oregon), separate the mainstem Klamath River into upper and lower basins (Figure 1). In the upper basin, the removal of the hydroelectric facilities will provide volitional fish passage and access to cold-water habitat. In the lower basin, dam removal will allow for more naturally dynamic flow and sediment transport conditions (Department of the Interior et al., 2012).

Data Collection and Analysis Methods

In this pilot study, UAS surveys were collected at three spatial scales in representative reaches selected for repeat monitoring. The reaches, selected using a basin-scale geomorphic map and associated land-surface parameters (Curtis and Benthem, 2022), are distributed longitudinally along the mainstem Klamath River corridor below Iron Gate Dam (Figure 1). The study reaches are densely vegetated, which presented challenges for planning UAS flights, but the coarse-grained nature of the exposed bed sediments was well-suited for DGS, which requires grains to be clearly resolved in the UAS imagery. The Portuguese Creek study reach was selected for a proof-of-concept study to investigate the correlation between surface roughness and DGS and to evaluate the feasibility of using surface roughness as a surrogate metric for grain size.

Table 1. Summary of 2022 UAS surveys (Curtis and Taylor, 2023) collected at 7 repeat monitoring sites (Figure 1) located along the mainstem Klamath River corridor below Iron Gate Dam, California.

Site Name	Site ID	Altitude	Camera	Date	Flight Start Time	Flight End Time	Flight Time	Flight Altitude (m)	Number of images (N)	Ground Control Points (N)
Iron Gate	IG	High	GR2	6/14/2022	10:57 PDT	11:44 PDT	0:47	60.6	108	9
R-Ranch	RR	High	GR2	6/14/2022	08:53 PDT	09:06 PDT	0:13	59.0	314	9
Klamath Community Center	KCC	High	GR2	6/16/2022	10:42 PDT	11:23 PDT	0:41	66.2	851	10
Brown Bear	BrBr	High	GR2	6/13/2022	12:33 PDT	13:23 PDT	0:50	63.6	581	9
Portuguese Creek	PC	High	GR2	6/10/2022	13:06 PDT	13:21 PDT	0:15	67.3	328	7
Ferry Point	FP	High	GR2	6/9/2022	12:06 PDT	12:28 PDT	0:22	63.3	495	10
Big Bar	BB	High	GR2	6/8/2022	11:44 PDT	12:33 PDT	0:49	74.5	482	9
Iron Gate	IG	Mid	GR3	6/14/2022	12:24 PDT	14:02 PDT	1:38	17.8	405	6
Klamath Community Center	KCC	Mid	GR3	6/16/2022	10:55 PDT	11:30 PDT	0:35	19.0	914	4
Brown Bear	BrBr	Mid	GR3	6/13/2022	12:53 PDT	13:24 PDT	0:31	18.4	785	5
Portuguese Creek	PC	Mid	GR3	6/10/2022	13:40 PDT	14:30 PDT	0:50	17.6	734	3
Big Bar	BB	Mid	GR3	6/8/2022	13:41 PDT	14:17 PDT	0:36	31.5*	716	3
Iron Gate	IG	Low	GR3	6/14/2022	12:50 PDT	13:43 PDT	0:53	3.09	733	5
Klamath Community Center	KCC	Low	GR3	6/16/2022	14:42 PDT	14:51 PDT	0:09	5.71	478	7
Brown Bear	BrBr	Low	GR3	6/13/2022	13:45 PDT	14:20 PDT	0:35	5.34	923	5
Portuguese Creek	PC	Low	GR3	6/10/2022	12:39 PDT	13:26 PDT	0:47	4.27	1228	5
Ferry Point	FP	Low	GR3	6/9/2022	15:05 PDT	15:42 PDT	0:37	9.24*	635	5
Big Bar	BB	Low	GR3	6/8/2022	14:42 PDT	14:57 PDT	0:15	3.50	393	5

*Different scale

UAS Surveys

In June of 2022, multi-scale UAS surveys were collected at three altitudes (high ~60 m, mid ~30 m, and low ~6 m) to determine the appropriate scale for repeat mapping of surface roughness and DGS analysis. In 7 study reaches (Table 1), UAS imagery was collected using a Ricoh GRII or Ricoh GRIII camera mounted on a 3DR Solo quadcopter. High-altitude imagery was collected using a Ricoh GRII camera. Mid- and low-altitude imagery was collected with a Ricoh GRIII camera. The raw imagery, point clouds, orthomosaics, and DEMs will be published separately (Curtis and Taylor, 2023). Because site conditions and data quality varied across the study reaches, not every reach has imagery and photogrammetric products for all three altitudes.

Ricoh GRII Camera Specifications

Focal Length = 18.3 mm
Image Width = 4928 pixels
Image Height = 3264 pixels
Sensor Size (width) = 23.7 mm
Sensor Size (height) = 15.7 mm
Pixel Size (width) = 0.0048 mm/pixel
Pixel Size (height) = 0.0048 mm/pixel

RicohGRIII Camera Specifications

Focal Length = 18.3 mm
Image Width = 6000 pixels
Image Height = 4000 pixels
Sensor Size (width) = 23.5 mm
Sensor Size (height) = 15.6 mm
Pixel Size (width) = 0.0039 mm/pixel
Pixel Size (height) = 0.0039 mm/pixel

Standard data collection methods for UAS-SfM photogrammetry (Over et al., 2021) were followed. For the high- and mid-altitude UAS surveys, two types of reference markers were used. Ground control points (GCPs) were used to georeference, align, and optimize the SfM photogrammetric models. Checkpoints (CPs) were used to validate the accuracy of the camera optimization. The GCPs and CPs were surveyed using autonomous Real-Time Kinematic Global Navigation Satellite System (RTK-GNSS) tiles (Aeropoints, Propeller Aerobotics Pty Ltd) that have a typical absolute horizontal accuracy of <2 cm and vertical accuracy of <5 cm. For the low-altitude surveys, calibrated scale bars with a precisely known length were used for scale. The scale bars had an absolute accuracy of <0.1 cm. The high- and mid-altitude datasets were published using a compound coordinate system (NAD83 (2011) UTM Zone10 + NAVD88 (meters)). The low-altitude datasets were published using a local coordinate system (meters).

Flight plans and ground control were predetermined to ensure efficient and high-quality data collection. Flight planning involved pre-determining the most efficient flight lines to achieve high-quality imagery for SfM photogrammetry. Variables included flight altitude, flight speed, grid pattern, imagery overlap and sidelap, camera focal length, sensor size, and camera trigger time. We used a nested approach to establish ground control and scale. The high-altitude surveys had nine or more GCPs and one CP, the mid-altitude surveys had three or more GCPs and one CP, and the low-altitude surveys had five or more scale bars.

SfM Photogrammetry

The multi-scale UAS imagery was post-processed using AgiSoft Metashape Professional 1.8.4. Standard SfM photogrammetry methods were used to build the DEMs and orthomosaics (Over et al., 2021). The post-processing workflow involves aligning overlapping images, adding ground control or scale, error reduction and optimization, and building and exporting the DEMs and orthomosaics at the appropriate resolution for analysis. The orthomosaics are image products orthorectified to correct for geometric distortion and color balanced to produce a seamless mosaicked product. The DEMs include all of the natural and human-made features (vegetation, structures, and bare ground) in the surveyed areas. The high-, mid-, and low-altitude DEMs and orthomosaics were exported at a common resolution to support comparison among monitoring sites (Table 1).

Surface Roughness

An ArcGIS Surface Roughness Toolbox was created to compute surface-roughness maps for the high-, mid-, and low-altitude surveys. The tools were used to create a grid, define centroids, compute and assign mean elevations to the grid centroids, interpolate a trend raster using the centroid elevations, and detrend the DEM by subtracting the trend raster to remove the reach slope and bedform gradients. There are many ways to compute surface roughness (Smith, 2014). In this study, surface roughness maps were computed using the standard deviation of detrended elevations (σ_z) within a 1-meter roughness grid (Smart et al., 2004; Brasington et al., 2012; Pearson et al., 2017, Bertin et al., 2018).

The surface-roughness maps provide a summary of topographic variability in vertical height units (meters). Because surface roughness is scale-dependent (Grohmann and Riccomini, 2009, Smith, 2014), the roughness heights computed for the high-, mid-, and low-UAS altitudes were different. We experimented with the size of the grid to optimize results. For determining grain-

scale roughness, the grid size should be at least 2.5 times the diameter of the largest particle (Smart et al., 2002). Due to the coarse-grained nature of the study site, a 1-meter grid was required to ensure adequate sampling of boulder-sized material (>256 mm).

Digital Grain Size

To investigate the correlation between surface roughness and DGS at the Portuguese Creek study site, we used a random number generator to select 12 of the 1-meter grid cells from the low-altitude-roughness grid. The twelve grid cells were exported as polygons and used to clip twelve 2D images for DGS analysis from the low-altitude orthomosaic. If vegetation was present in the randomly selected plot, an adjacent plot was selected in a clockwise manner starting with the upper left plot.

For the DGS analysis, we used "pyDGS", an open-source Python code (Buscombe, 2013) that estimates grain-size percentiles (5, 10, 16, 25, 32, 75, 84, 90, 95) and grain-size statistics (mean, sorting, skewness, kurtosis) directly from 2D images of sediment with the grains clearly resolved. The code, pyDGS, uses a Morlet wavelet method to estimate a grain-size distribution that is equivalent to grid-by-number methods (Bunte and Abt, 2001). The method involves wavelet transformation and decomposition of an image of sediment into variance as a function of frequency to identify individual grains. Although pyDGS requires scaling, site-specific calibration is not required, and the code can be run in batch mode; pyDGS is best suited for measuring relative differences in grain size within or among sites. The resolution of the orthomosaic constrains the minimum measurable grain size, and smaller grains may be hidden beneath larger grains. For these reasons, pyDGS tends to overestimate the grain-size percentiles.

Results

The influence of scale on surface roughness is captured by the high-, mid-, and low-altitude UAS surveys at the Portuguese Creek study site (Figures 2 and 3). Higher-altitude roughness values had smaller roughness heights. Coarser patches of sediment (Figure 2) had larger roughness heights, and finer patches of sediment (Figure 3) had lower roughness heights. The surface-roughness maps provided grain-scale detail at all three spatial scales. The mid-altitude survey provided orthomosaics suitable for heads-up digitizing of coarse- and fine-sediment facies. The low-altitude survey provided hyper-resolution (1.5 to 2.5 mm) orthomosaics suitable for DGS of fine-gravel particles ≥ 8 mm. At the reach scale, variations in grain size were readily apparent in the low-altitude roughness map (Figure 4).

Dense vegetation along the channel margin obscured much of the area of interest, complicating efforts to select plots for DGS. The Portuguese Creek site was the only site with UAS datasets suitable for DGS, which requires 2D imagery with clearly visible and well-resolved grains. Although pyDGS cannot resolve subpixel grain, only a few pixels per grain are required for analysis. The low-altitude orthomosaic had a 1.5 mm resolution (Table 2), and pyDGS truncates the grain size distribution at the 5^{th} percentile.

The Portuguese Creek regression models showed statistically significant correlations ($p<0.0001$) between surface roughness, computed using the low-altitude DEM, and two DGS metrics representing the 50^{th} (D50) and 84^{th} percentile (D84), computed using plot data clipped from

the low-altitude orthomosaic (Figure 6). This result indicates that surface roughness can be used as a surrogate metric for grain size. Although vegetation encroachment complicated efforts to select plots for DGS analysis, the surface-roughness measurements provided accurate grain-scale information, further demonstrating the applicability of using surface roughness as a surrogate metric for grain size.

Table 2. Summary of SfM photogrammetric products derived from 2022 UAS surveys collected at 7 repeat monitoring sites (Figure 1) located along the mainstem Klamath River corridor below Iron Gate Dam, California.

Site Name	Site ID	Altitude	Surveyed Area (m^2)	Checkpoint Error (cm)	Reprojection Error (pixel)	Root Mean Squared Error (cm)	Ortho Native Resolution (mm)	DEM Native Resolution (mm)	Exported Ortho Resolution (mm)	Exported DEM Resolution (mm)
Iron Gate	IG	High	5,650	2.78	0.20	1.60	12.1	24.1	20	40
R-Ranch	RR	High	134,000	4.06	0.18	8.90	14.8	29.6	20	40
Klamath Community Center	KCC	High	189,000	4.49	0.19	10.1	13.2	26.4	20	40
Brown Bear	BrBr	High	86,200	5.80	0.19	4.34	17.9	35.7	20	40
Portuguese Creek	PC	High	53,700	2.18	0.21	3.26	15.7	31.3	20	40
Ferry Point	FP	High	194,000	2.57	0.19	4.24	14.7	29.3	20	40
Big Bar	BB	High	176,000	2.78	0.19	1.39	18.4	36.9	20	40
Iron Gate	IG	Mid	2,600	3.42	0.19	1.93	3.44	6.89	4	8
Klamath Community Center	KCC	Mid	10,800	22.6	0.21	1.02	3.80	7.61	4	8
Brown Bear	BrBr	Mid	9,690	1.00	0.21	2.94	3.44	6.89	4	8
Portuguese Creek	PC	Mid	6,980	9.00	0.24	1.18	3.44	6.88	4	8
Big Bar	BB	Mid	17,400	9.43	0.34	0.76	6.65	13.3	7.5*	15*
Iron Gate	IG	Low	439	0.05	0.22	0.21	0.63	1.26	1.5	3
Klamath Community Center	KCC	Low	1,330	0.02	0.22	0.04	1.27	2.54	1.5	3
Brown Bear	BrBr	Low	755	0.02	0.23	0.21	1.05	2.11	1.5	3
Portuguese Creek	PC	Low	1,170	0.04	0.19	0.04	0.86	1.72	1.5	3
Ferry Point	FP	Low	1,860	0.48	0.18	0.80	1.92	3.83	2.5*	5*
Big Bar	BB	Low	644	0.05	0.21	0.03	0.73	1.45	1.5	3

*Different resolution

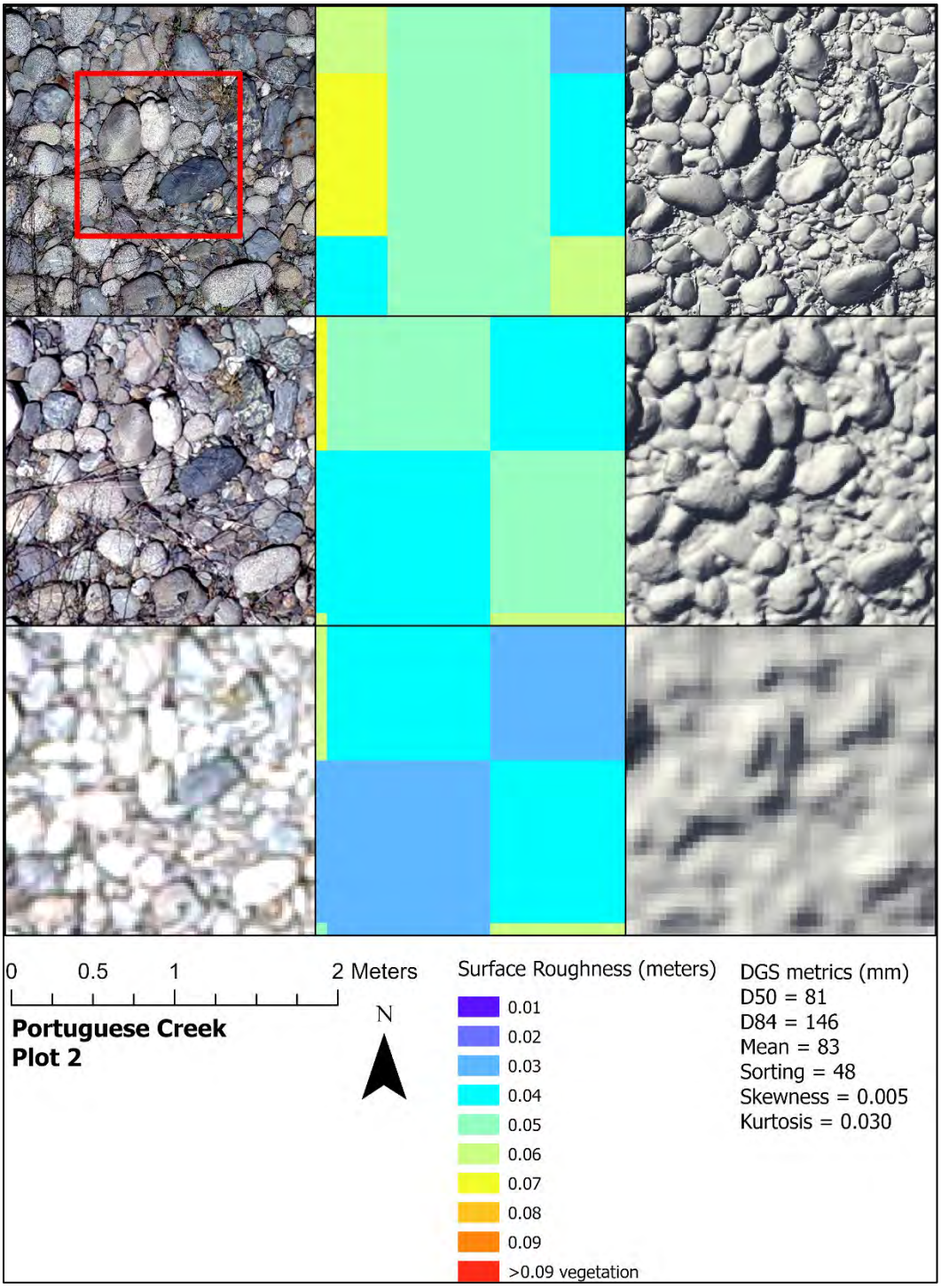

Figure 2. Low-, mid-, and high-altitude orthomosaics, surface roughness maps, and hillshades showing grain-scale detail for plot PC2 (Figure 4) at the Portuguese Creek study site (Table 2) located along the mainstem Klamath River corridor below Iron Gate Dam, California (Figure1). The DGS plot is shown with a red outline. Smaller roughness heights (cool colors) correlate to finer sediment and larger roughness heights (warm colors) correlate to coarser sediment. Roughness values >0.09 (red) correlate to vegetation. The grid alignment is controlled by the coordinate system and the horizontal errors (Table 2).

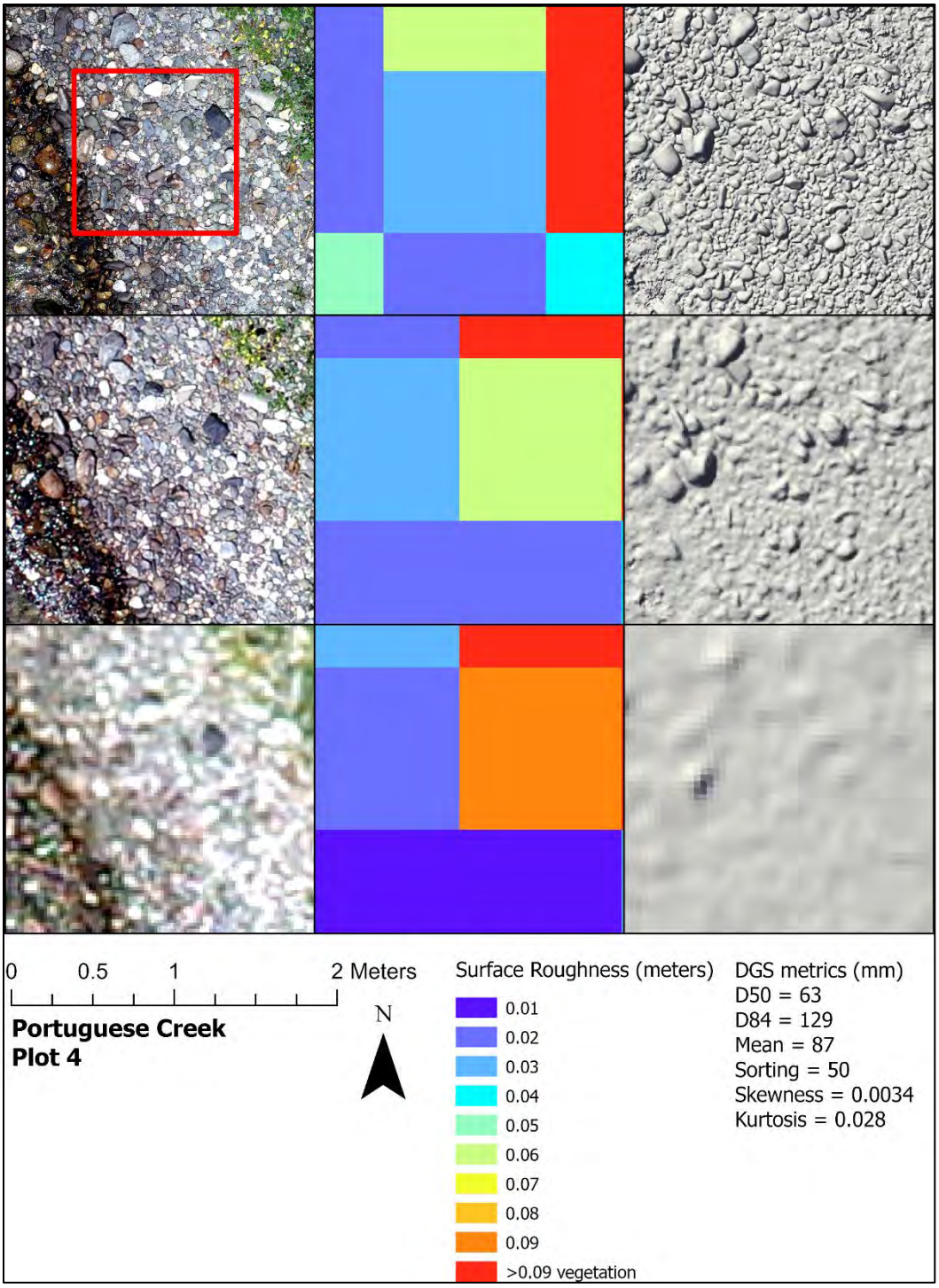

Figure 3. Low-, mid-, and high-altitude orthomosaics, surface roughness maps, and hillshades showing grain-scale detail for plot PC4 (Figure 4) at the Portuguese Creek study site (Table 2) located along the mainstem Klamath River corridor below Iron Gate Dam, California (Figure1). The DGS plot is shown with a red outline. Smaller roughness heights (cool colors) correlate to finer sediment and larger roughness heights (warm colors) correlate to coarser sediment. Roughness values >0.09 (red) correlate to vegetation. The grid alignment is controlled by the coordinate system and the horizontal errors (Table 2).

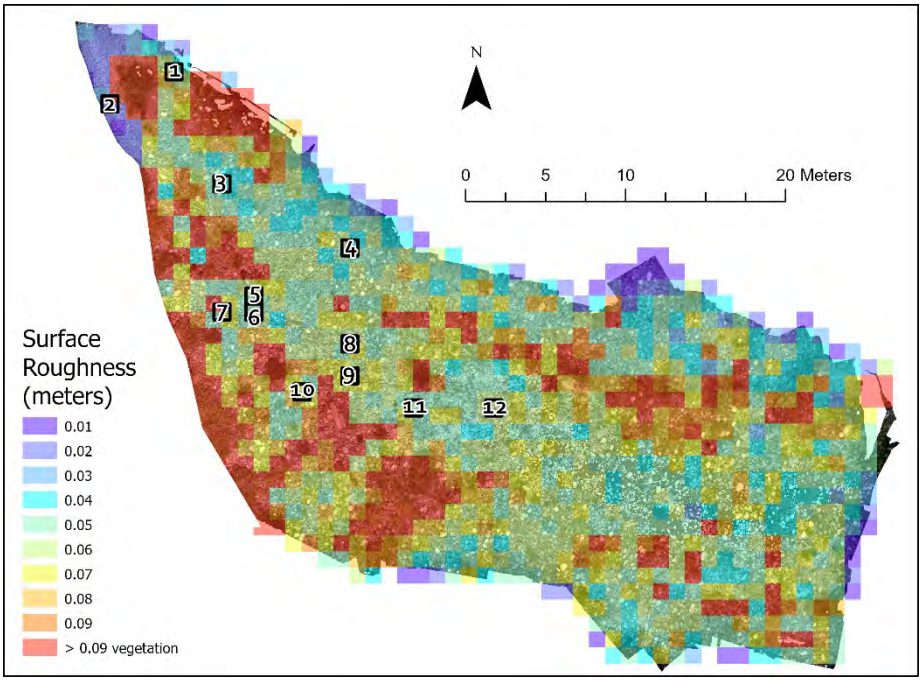

Figure 4. Low-altitude orthomosaic and classified roughness map (50% transparent) showing grain-scale roughness, in meters, over a reach-scale extent and the location of the twelve DGS plots at the Portuguese Creek study site (Table 2) located along the mainstem Klamath River corridor below Iron Gate Dam, California (Figure1). Smaller roughness heights (cool colors) correlate to finer sediment and larger roughness heights (warm colors) correlate to coarser sediment. Roughness values >0.09 (red) correlate to vegetation.

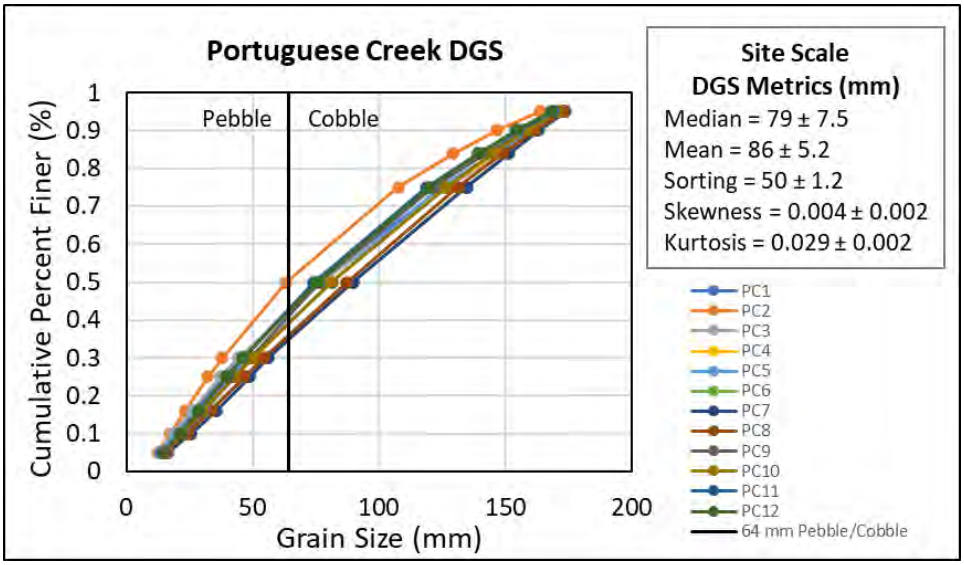

Figure 5. Digital grain size distributions (Table 3) computed using pyDGS (Buscombe, 2013) for 12 plots at the Portuguese Creek study site (Table 2) located along the mainstem Klamath River corridor below Iron Gate Dam, California (Figure 1).

Table 3. Summary of surface roughness, digital grain size percentiles, and statistical metrics related to grain size for the Portuguese Creek study site (Figure 1) located along the mainstem Klamath River corridor below Iron Gate Dam, California.

	Digital Grain Size Percentiles (mm)										Statistical Metrics			
Plot	5	10	16	25	32	50	75	84	90	95	mean	sorting	skewness	kurtosis
PC1	13.6	19.9	27.2	38.1	44.7	75.2	125.9	146.6	160.9	172.7	84.6	51.2	0.005	0.028
PC2	12.3	17.3	23.1	32.2	37.9	63.2	107.5	129.2	146.4	163.5	87.3	49.6	0.003	0.028
PC3	12.6	18.5	25.9	37.2	44.1	77.2	127.1	147.5	161.1	172.5	82.6	48.5	0.006	0.031
PC4	14.0	21.3	29.6	42.8	50.3	80.9	126.1	146.4	160.3	172.1	83.0	48.5	0.005	0.030
PC5	13.7	20.3	28.2	41.0	48.7	81.4	124.2	145.3	159.9	172.0	74.3	47.5	0.008	0.034
PC6	15.6	23.4	32.3	46.9	55.6	89.4	134.3	151.2	163.3	173.8	85.0	51.8	0.004	0.028
PC7	16.5	25.7	35.4	48.8	56.0	89.6	134.5	151.1	162.9	173.3	87.2	50.0	0.004	0.029
PC8	15.9	24.0	33.2	46.6	54.2	87.2	131.2	148.7	161.4	172.7	86.5	50.1	0.004	0.029
PC9	15.4	22.5	30.7	42.6	49.0	76.5	121.5	142.0	156.7	169.8	92.8	50.7	0.001	0.027
PC10	14.7	21.6	29.8	42.6	49.9	81.4	126.6	144.8	158.3	170.7	93.4	50.0	0.002	0.027
PC11	14.3	21.0	28.5	39.7	46.2	74.1	118.6	139.1	154.7	169.0	91.3	49.8	0.002	0.028
PC12	14.4	21.0	28.5	39.5	46.0	75.3	119.9	139.3	153.9	167.8	84.8	48.5	0.005	0.030

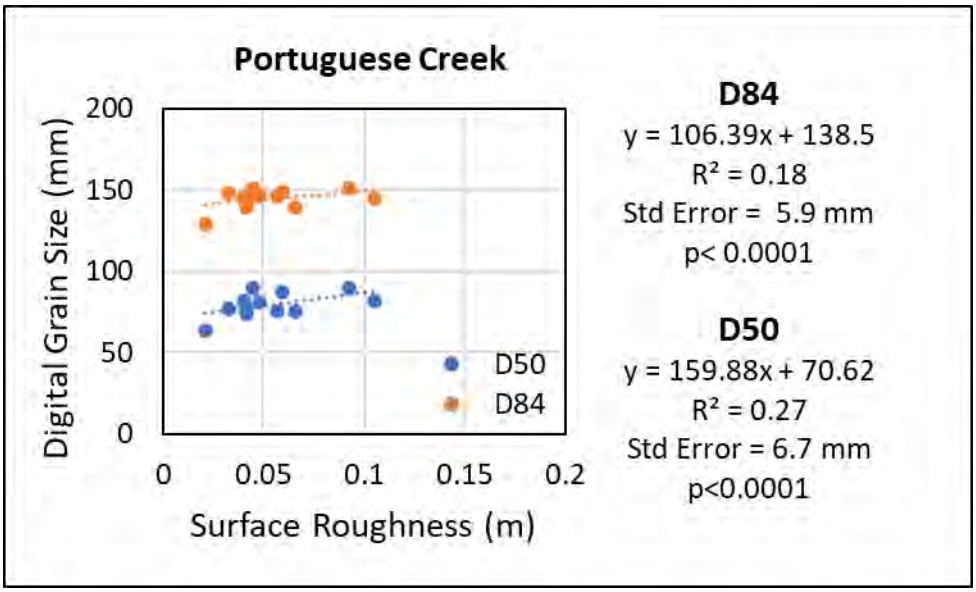

Figure 6. Regression models showing the statistical correlation between surface roughness and statistical metrics related to grain size (D50 and D84) derived from low-altitude UAS imagery collected at the Portuguese Creek study site (Figure 1) located along the mainstem Klamath River corridor below Iron Gate Dam, California.

Discussion

In this study, we evaluated the use of UAS-SfM photogrammetry methods for mapping surface roughness and DGS on exposed alluvial bars along the mainstem Klamath River. Numerous studies have shown a strong correlation between surface roughness and grain size (Smart et al 2004, Brasington et al, 2012; Westoby et al., 2015; Pearson et al. 2017, Bertin et al 2018). The

strength of the correlation depends upon the scale of the analysis and the quality of the imagery. Challenges in this study that influenced the accuracy of the DEMs and orthomosaics included environmental conditions (lighting, wind), image quality (shadows, exposure, saturation, and contrast), and densely vegetated channel margins that limited the exposed areas suitable for DGS.

Study results indicate that UAS mapping can be used for rapid assessment of surface roughness and DGS in exposed areas of the river corridor. At the plot scale, surface roughness and DGS values were positively correlated indicating surface roughness can be used as a surrogate metric for grain size. The regression models had low R^2 values indicating low predictive power (Figure 5; Helsel et al., 2020). For this reason, the regression models cannot be used to compute reach-scale estimates of grain size from roughness heights. The range of D50 and D84 values in the correlation analysis was narrow in comparison to the range of roughness heights and this may have influenced the quality of the surface roughness and DGS regression analysis. Future work will focus on sampling a wider range of grain sizes across multiple study reaches to improve the statistical correlation between roughness heights and DGS metrics.

The DGS methods used in this study are most appropriate for rapid assessment of relative differences in the grain size of bed sediments, rather than computing absolute estimates of grain size. When extracting plots from orthomosaics derived from UAS surveys, the sample size is easily increased to improve accuracy and reduce uncertainty with a relatively small increase in analysis time. As suggested by Buscombe (2013), a sample size of around 250 grains per image is required to achieve a root mean square error of around 20% or less. The number of grains sampled in each plot is also easily increased by increasing the size of the plot, and the total sampled area is easily increased by increasing the number of plots per site. In cases where roughness heights and DGS are strongly correlated, each cell of a roughness map can be treated as a separate grain-size sample and a regression model with higher predictive power could be used to compute reach-scale, grain-size statistics.

Navigation, aircraft shadows, propeller wash, and variable lighting conditions were problematic for low and slow UAS surveys. We encountered navigation problems related to the lack of onboard high-precision GPS, which makes low and slow navigation difficult. Periodically we also encountered multipath problems related to the GPS signal bouncing off of nearby objects and steep surrounding topography. Improved UAS navigation features, such as post-processed kinematic (PPK) GPS and obstacle avoidance, would greatly improve the ability to fly low and slow UAS surveys for DGS analysis and would improve the overall quality of low-altitude UAS imagery and photogrammetric products. Surveying so close to the ground surface produced aircraft shadows in the imagery, and propeller wash caused fine sediment to become airborne and impact image quality.

Due to the fine-grained nature of the reservoir sediments and the coarse-grained nature of the downstream river corridor, UAS-SfM photogrammetry and DGS are particularly well-suited for monitoring the downstream effects of Klamath River dam removals. During and following dam removal, increases in fine-sediment flux may cause temporary bed fining. Aerial LiDAR, with a typical spatial resolution of 1 meter, and imagery collected from crewed aircraft will be useful for monitoring morphologic changes in the primary response reach close to the dams. However, higher-resolution, pixel-based methods are required to detect changes in bed textures and for DGS analysis on exposed alluvial bars.

In this study, the combination of UAS-SfM photogrammetry and DGS analysis produced hyper-resolution datasets for exposed areas of the river corridor. Repeat UAS surveys will provide a

fundamental understanding of fluvial processes (deposition and erosion) and river hydraulics (grain sorting and surface flushing of fine sediment) that can be used to investigate the influence of changes in flow, sediment supply, and human activities on the textural characteristics of exposed bed sediments. UAS-SfM photogrammetry and DGS methods will continue to be evaluated as part of ongoing Klamath River dam removal studies.

Conclusions

This study evaluated the use of Uncrewed Aircraft System (UAS) for mapping surface roughness and digital grain size (DGS) along the mainstem Klamath River corridor below Iron Gate Dam, California. Photogrammetric products with grain-scale detail for reach-scale extents were produced using methods that are fast, non-destructive, repeatable, and transferable. Surface roughness, computed as the standard deviation of detrended bed elevations, is scale-dependent. Defining the appropriate scale and resolution for successful data collection is a critical consideration. The high-altitude UAS surveys provided digital elevation models (DEMs) suitable for mapping surface roughness. The mid-altitude surveys provided DEMs and orthomosaics suitable for heads-up digitizing of coarse- and fine-sediment facies. The Portuguese Creek low-altitude survey provided DEMs and orthomosaics with the grains clearly resolved and suitable for DGS analysis. Surface roughness is a suitable surrogate metric for grain size. The methods used in this study are most appropriate for assessing relative differences in bed textures and grain size, rather than computing absolute estimates of grain size. The close-range, remote-sensing methods evaluated in this proof-of-concept study can be used for rapid assessment of textural changes and characterization of bed fining in exposed areas of the river corridor during and following Klamath River dam removal.

U.S. Geological Survey Disclaimers

Any use of trade, firm, or product names is for descriptive purposes only and does not imply endorsement by the U.S. Government. These data are preliminary or provisional and are subject to revision. They are being provided to meet the need for timely best science. The data have not received final approval by the U.S. Geological Survey (USGS) and are provided on the condition that neither the USGS nor the U.S. Government shall be held liable for any damages resulting from the authorized or unauthorized use of the data.

References

Bertin, S., Groom, J. and Friedrich, H., 2018, September. Grain and bedform roughness properties isolated from gravel-patch DEMs. In RiverFlow 2018 (Vol. 40).

Brasington, J., Vericat, D. and Rychkov, I., 2012. Modeling river bed morphology, roughness, and surface sedimentology using high resolution terrestrial laser scanning. Water Resources Research, 48(11). https://doi.org/10.1029/2012WR012223

Bunte, K., and Abt, S.R., 2001, Sampling surface and subsurface particle-size distributions in wadable gravel- and cobble-bed streams for analyses in sediment transport, hydraulics, and streambed monitoring: Fort Collins, Colo., U.S. Department of Agriculture, Forest Service, Rocky Mountain Research Station, General Technical Report RMRS-GTR-74, 428 p. https://www.fs.fed.us/rm/pubs/rmrs_gtr074.pdf

Buscombe, D., 2013. Transferable wavelet method for grain-size distribution from images of sediment surfaces and thin sections, and other natural granular patterns. Sedimentology, 60(7), pp.1709-1732. https://doi.org/10.1111/sed.12049

Chen, X., Hassan, M.A., An, C. and Fu, X., 2020. Rough correlations: Meta-analysis of roughness measures in gravel bed rivers. Water Resources Research, 56(8), p.e2020WR027079. https://doi.org/10.1029/2020WR027079

Curtis, J.A., Poitras, T.B., Bond, S.B., and Byrd, K.B., 2021, Sediment mobility and river corridor assessment for a 140-km segment of the main stem Klamath River below Iron Gate Dam, CA: U.S. Geological Survey Open-File Report 2020-1141. https://doi.org/10.3133/ofr20201141

Curtis, J.A. and Benthem, A.J., 2022, Baseline geomorphic map and land-surface parameters, derived from integrated topobathymetric elevation data, for the mainstem Klamath River corridor downstream of Iron Gate Dam, CA, 2018: U.S. Geological Survey data release. https://doi.org/10.5066/P90KEKPH

Curtis, J.A. and Taylor, J.J. 2023, Aerial imagery and structure-from-motion data products from pre-dam removal UAS surveys along the mainstem Klamath River corridor downstream from Iron Gate Dam, CA, 2022, U.S. Geological Survey Data Release. https://doi.org/10.5066/P9NFKASP

Department of the Interior, Department of Commerce, and National Marine Fisheries Service, 2012, Klamath Dam removal overview report for the Secretary of the Interior–An assessment of science and technical information (version 1.1): U.S. Fish and Wildlife Service. https://www.fws.gov/arcata/fisheries/reports/technical/Full%20SDOR%20accessible%20022216.pdf

Grohmann, C.H. and Riccomini, C., 2009. Comparison of roving-window and search-window techniques for characterizing landscape morphometry. Computers & Geosciences, 35(10), pp.2164-2169. https://doi.org/10.1016/j.cageo.2008.12.014

Groom, J., Bertin, S. and Friedrich, H., 2019. Moving-Window Detrending for Grain-Roughness Parameterization. Journal of Hydraulic Engineering, 145. https://doi.org/10.1061/(ASCE)HY.1943-7900.0001612

Helsel, D.R., Hirsch, R.M., Ryberg, K.R., Archfield, S.A., and Gilroy, E.J., 2020, Statistical methods in water resources: U.S. Geological Survey Techniques and Methods, book 4, chap. A3, 458 p., https://doi.org/10.3133/tm4a3. [Supersedes USGS Techniques of Water-Resources Investigations, book 4, chap. A3, version 1.1.]

Hey, R.D., 1979. Flow resistance in gravel-bed rivers. Journal of the Hydraulics Division, 105(4), pp.365-379. https://doi.org/10.1061/JYCEAJ.0005178

Holmquist-Johnson, C.L., and Milhous, R.T., 2010, Channel maintenance and flushing flows for the Klamath River below Iron Gate Dam, California: U.S. Geological Survey Open-File Report 2010–1086, 31 p., https://doi.org/10.3133/ofr20101086

Lane, S.N., 2005. Roughness-time for a re-evaluation?. Earth Surface Processes and Landforms, 30(2), pp.251-253. https://doi.org/10.1002/esp.1208

Over, J.R., Ritchie, A.C., Kranenburg, C.J., Brown, J.A., Buscombe, D., Noble, T., Sherwood, C.R., Warrick, J.A., and Wernette, P.A., 2021, Processing coastal imagery with Agisoft Metashape Professional Edition, version 1.6—Structure from motion workflow documentation: U.S. Geological Survey Open-File Report 2021–1039, 46 p. https://doi.org/10.3133/ofr20211039

Pearson, E., Smith, M.W., Klaar, M.J. and Brown, L.E., 2017. Can high resolution 3D topographic surveys provide reliable grain size estimates in gravel bed rivers?. Geomorphology, 293, pp.143-155. https://doi.org/10.1016/j.geomorph.2017.05.015

Powell, D.M., 2014. Flow resistance in gravel-bed rivers: Progress in research. Earth-Science Reviews, 136, pp.301-338. https://doi.org/10.1016/j.earscirev.2014.06.001

Reclamation, 2011, Hydrology, Hydraulics, and Sediment Transport Studies for the Secretary's Determination on Klamath River Dam Removal and Basin Restoration, Technical Report No. SRH-2011-02. Prepared for Mid-Pacific Region, US Bureau of Reclamation, Technical Service Center, Denver, CO.

Smart, G.M., Duncan, M.J. and Walsh, J.M., 2002. Relatively rough flow resistance equations. Journal of Hydraulic Engineering, 128(6), pp.568-578. https://doi.org/10.1061/(ASCE)0733-9429(2002)128:6(568)

Smart, G., Aberle, J., Duncan, M. and Walsh, J., 2004. Measurement and analysis of alluvial bed roughness. Journal of Hydraulic Research, 42(3), pp.227-237. https://doi.org/10.1080/00221686.2004.9728388

Smith, M.W., 2014. Roughness in the earth sciences. Earth-Science Reviews, 136, pp.202-225. https://doi.org/10.1016/j.earscirev.2014.05.016

van Rijn, L.C., 1982, Equivalent Roughness of Alluvial Bed, ASCE Journal of Hydraulic Engineering, 108 (10), pp. 1215-2018. https://doi.org/10.1061/JYCEAJ.0005917

Westoby, M.J., Brasington, J., Glasser, N.F., Hambrey, M.J. and Reynolds, J.M., 2015. 'Structure-from-Motion'photogrammetry: A low-cost, effective tool for geoscience applications. Geomorphology, 179, pp.300-314. https://doi.org/10.1016/j.geomorph.2012.08.021

Wolman, M.G., 1954. A method of sampling coarse river-bed material. EOS, Transactions American Geophysical Union, 35(6), pp.951-956. https://doi.org/10.1029/TR035i006p00951